First International Conference
Modelling and Development of Intelligent Systems
Sibiu - Romania, 22-25 October, 2009

Automated contour determination in ultrasound medical images

Vera Behar, Pavlina Konstantinova, Milen Nikolov

Abstract

Contour determination in images is often the main goal in image utilization. There is no universal segmentation algorithm for images acquired by different technologies in different practical applications. The developed contour tracking algorithm, which is a combination of probabilistic data association approach and Interacting Multiple Model approach, shows attractive results for successful contour determination. This algorithm is based on the assumption that the lesion has convex form, which is often true in medical images. The developed algorithm is forced by equally spaced radii from a pre-defined seed point inside the lesion area. A disadvantage of this method is that this point must be selected manually by the user. In this paper an algorithm for automated selection of the internal seed point is proposed. It is supposed that the image intensity can be divided into two classes of intensities: one - for the background and the other - for the lesion. The main idea is to convert the image in a binary form using appropriate thresholding. Then the pixels of the lesion class are processed to find the center of gravity of the lesion area. This center is assumed to be the required seed point.

1 Introduction

In recent years ultrasound imaging is widely used in different practical applications. It is non-invasive, suitable for real time applications and has comparatively low cost. Contour determination in images is often the main goal in image utilization. There is no universal segmentation algorithm for images acquired by different technologies in different practical areas of application. Usually some prior information is used to make possible an effective solution of the segmentation problem. In [9], an extensive research of the ultrasound medical image segmentation methods is presented. The authors classify the considered methods by their clinical applications. This is motivated by the fact that some specific image characteristics like the convex form of the medical structures or other peculiarities are taken into account. The final paper of the survey in the ten selected influential works is that of Abolmaesumi and Sirospour [1]. The authors developed cavity boundary extraction algorithm based on the known tracking algorithm intended for tracking maneuvering targets in clutter. The algorithm combines the advantages of two powerful approaches- probabilistic data association (PDA) approach and Interacting Multiple Model approach. The algorithm is forced by the equally spaced radii from a

pre-defined seed point inside the lesion area [1]. It incorporates the edge magnitude in probabilistic data association to find a more appropriate point of the contour.

In [2], a new efficient multiple model Monte Carlo algorithm is developed for progressive contour tracking, which takes into account convex, non-circular forms of the lesion areas for segmentation. Another realization of idea proposed in [1] is developed in [6] and [8]. In [8], a new feature, based on the statistical mean intensity of the region around the predicted contour point (pixel) is used to modify the weights of the candidate pixels and to improve the reliability of the tracking process.

The contour determination algorithms based on the tracking idea, show attractive results for successful contour determination. Their common property is the necessity of an internal seed point, which is usually selected manually by the user.

The goal of this paper is to fully automate the segmentation process by automatically selecting the internal seed point. It is supposed that the image contains two classes of intensities: one for the background and the other - for the lesion. The main idea is to convert the image in a binary form using appropriate thresholding. Then the pixels of the lesion class in the binary image are processed to find the center of gravity of the lesion area. This center is assumed to be the required seed point.

The paper is organized as follows. After the introduction the problem of contour determination by using the tracking algorithm is formulated. The proposed algorithm for determination of the internal seed point is presented in section 3. In section 4 the results of using the proposed algorithm are given on the base of both modeled and real ultrasound medical images. In section 5 conclusions are given.

2 Problem Formulation

In medical images the cysts and other lesions more often have a convex form. This property allows the following assumption - the contour of interest is star-shaped i.e. all contour points can be seen from an appropriately selected seed point inside the assumed contour. The contour determination algorithm developed in [1, 6, 8] uses PDA and IMM approaches for tracking of low observable maneuvering target in the presence of false alarms [12]. The contour is treated as a target trajectory and the contour points are defined on the equally spaced radii from the selected seed point inside the assumed contour.

The system state vector x, describing the target dynamic evolves in time according to

$x(k+1) = F(k)x(k) + \nu(k),$ with the measurement vector z, given by:

$z(k+1) = H(k)x(k) + \omega(k)$, where F is the system transition matrix, H is the measurement matrix, $\nu(k)$ and $\omega(k)$ are the zero-mean mutually independent white Gaussian noise sequences with the known covariance matrices $Q(k)$ and $R(k)$, respectively, and k is the time sample.

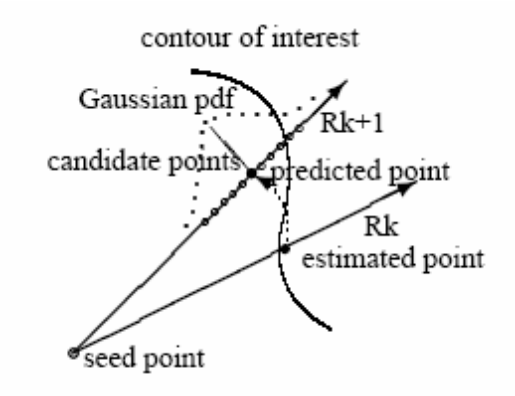

Fig .1. Scheme of the algorithm using seed point

The system dynamic is forced by the equally spaced radii. The schematic presentation of this formulation is shown in figure 1, where two consecutive radii R_k and R_{k+1} are presented. The estimated point is located on the radius R_k and the corresponding predicted point is located on the radius R_{k+1}. The candidate points around the predicted point with their Gaussian pdf associated with the assignment of the corresponding point to the trajectory of the contour are also presented.

The state vector is $x = \left[D \quad \dot{D}\right]'$, where D is the distance from the seed point to the current point and $\dot{D} = \frac{dD}{d\theta}$. The increment of the angle $\Delta\theta = 2\pi / \mathrm{N_r}$, N_r is the number of radii that corresponds to the number of the evaluated contour points. For more details see [3, 12, 6].

3 Automated determination of the internal seed point

The algorithm for automatic determination of the seed point is developed under the following assumptions:

- The image intensity consists of two main classes of intensities – for the object and for the background;
- Only one object is located in the processed region of interest;

The algorithm includes the following processing steps:

1. Select the appropriate threshold with the Otsu algorithm;
2. Form the binary image using the determined threshold;
3. Find the center of gravity of the pixels, corresponding to the class of intensities that characterizes the object. This center is the desired internal point.

The first important step in this algorithm is to select the appropriate threshold. The algorithm developed by Otsu in [7] can be used for this purpose. It seems to be suitable for the case of two classes of pixels. The Otsu algorithm minimizes the weighted sum of within-class variances of the object and background pixels, which is equivalent to maximization of between-class variance. This fact proves the optimality of the determined threshold.

Otsu algorithm description according to [7]

Lets represent the intensities of the image by L gray levels {0,1,2,…L-1} The number of pixels of the level i is denoted by h_i and the total number of pixels is denoted by N. The gray level histogram is normalized and is regarded as a probability distribution function:

$$p_i = h_i / N, \qquad p_i >= 0, \qquad \sum_{i=0}^{L-1} p_i = 1 \ .$$

We assume that the pixels can be divided into two classes C_0 and C_1 by a threshold of the intensity k. Class C_0 includes pixels with the intensity levels {0,1,…,k} and C_1 includes pixels with the intensity levels {k+1,k+2,…,L-1}.

The definition of these classes depends on the lesion types:

- For lesions of type "Cyst" – the objects are darker than the background i.e. the objects are of class C_0 and the background – of class C_1;
- For lesions of type "Tumor" – the objects are lighter than the background i.e. the objects are of class C_1 and the background – of class C_0;

The probabilities for class occurrences ω and the class mean levels μ for both classes are given for each k by:

$$\omega_0(k) = \sum_{i=0}^{k} p_i \ , \qquad \omega_1(k) = \sum_{i=k+1}^{L-1} p_i = 1 - \omega_0(k),$$

$$\mu_0(k) = \sum_{i=0}^{k} i \times p_i / \omega_0(k), \qquad \mu_1(k) = \sum_{i=k+1}^{L-1} i \times p_i / \omega_1(k) = \frac{\mu_{tot} - \mu_k(k)}{1 - \omega_0(k)},$$

where $\mu_k(k) = \sum_{i=0}^{k} i \times p_i$ and the total mean $\mu_{tot} = \sum_{i=0}^{L-1} i \times p_i$.

The class variances are:

$$\sigma_0^2(k) = \sum_{i=0}^{k} (i - \mu_0(k))^2 \, p_i \quad , \sigma_1^2(k) = \sum_{i=k+1}^{L-1} (i - \mu_1(k))^2 \, p_i = \sigma_{tot}^2 - \sigma_0^2(k) \quad ,$$

where the total standard deviation is $\sigma_{tot}^2 = \sum_{i=0}^{L-1} (i - \mu_{tot})^2 \, p_i$.

Otsu suggested the minimization of the weighted sum of within-class variances of both the object and the background pixels to establish the optimal threshold. Recall that the minimization of within-class variances is equivalent to the maximization of between class variance. For each intensity k, the between class variance can be evaluated by:

$\sigma_B^2(k) = \omega_0(k)(\mu_0(k) - \mu_{tot})^2 + \omega_1(k)(\mu_1(k) - \mu_{tot})^2$.

The optimal threshold is defined as $k_{opt} = \max_k \{\sigma_B^2\}$.

Auxiliary binary image

The auxiliary binary image is obtained by using the array of intensities of the original image $Org\,\mathrm{Im}$ and the optimal threshold k_{opt} . Then the binary image array, which is previously cleaned by zeros, is formed as follows:

if $Org\,\mathrm{Im}(i,j) > k_{opt}$ $Bin\,\mathrm{Im}(i,j) = 1$; for i=1...N ; j=1...M , where NxM is the image size.

The binary $Bin\,\mathrm{Im}$ array is used to find the center of gravity of the pixels of the object class. The center of gravity (x_o, y_o) (or center of mass with uniformly distributed masses of the pixels) is obtained by:

$$x_o = \frac{\sum_{y=1}^{N}\sum_{x=1}^{M} x \quad for\ I(y,x)\in C_{obj}}{K} \quad \text{and} \quad y_o = \frac{\sum_{y=1}^{N}\sum_{x=1}^{M} y \quad for\ I(y,x)\in C_{obj}}{K},$$

where K is the number of the pixels $I(x,y)$ belonging to the object class C_{obj} .

This center is used as the internal seed point in the tracking algorithm for contour determination.

Image denoising

In some cases, prior the contour determination algorithm it is useful to perform the preprocessing - denoising procedure in order to reduce speckle noise. In our case we use a wavelet technique that provides an appropriate basis for noisy signal processing. The justification is that the wavelets transform the signals in the *time - frequency* domain [11, 13]. It is stated that in the frequency domain a small number of coefficients represent the significant information and a large number of coefficients with small values is supposed to represent the noise. Because of the multiplicative nature of the speckle noise a logarithmic transform is applied to transform multiplicative speckle noise to additive noise [10]. In [10] and also in our recent works we find out that dual-tree complex wavelet algorithm, developed and described by Kingsbury and Selesnick in [11, 13], gives the best results for contour detection. After wavelet coefficients thresholding the inverse logarithmic transform gives the smoothed image array.

4 Illustrative examples for automated determination of the seed point

Reliable tests of the described algorithm for automated determination of the seed point can be received by using simulated ultrasound images obtained by the Simulation program Field II [4, 5]. In

order to make our test more thoroughly we apply the algorithm to different forms of the objects. In addition we put together the results obtained for the original image and that after denoising.

One simulated image containing an elliptical tumor is presented on fig. 2a. A binary image produced from the simulated image by using the thresholding technique is shown on fig. 2b. On the same fig. 2b, the center of gravity of the pixels from the lesion object class is represented by little circle (in the center of the tumor). The estimated contour around the tumor (white line) is presented in fig. 2c. The true contour of the modeled object is presented by the black line. On fig. 3, the histogram of the intensities of the simulated image is presented and the determined threshold is marked on the x-axes with the symbol 'x'. In this case the threshold is 148, which means that the pixels with intensity greater than the threshold (148) are classified as pixels of the object (lighter than the background).

On fig. 4, the errors of the modeled contour are presented. The errors along axes x and y are presented by the thin lines, and the summarized distance error is presented by the bold line. It can be seen that only a few part of the contour points have error greater than 1 [mm].

The simulated image (from fig. 2a) is firstly denoised, and then the same processing algorithm is applied to the resultant image. The successful determination of the internal seed point is shown in fig. 5b and the outlined contour (white line) can be seen on fig. 5c. The errors shown on fig. 7 are decreased in comparison with the ones on fig. 4. The histogram on fig. 6 shows the increased difference between the centers of intensity of the two classes in comparison with the non-denoising case on fig. 3.

The more complicated form of the Oval Cassini is used to model another object. On fig. 8a, a modeled image with a tumor in form of the Oval Cassini is presented. The auxiliary binary image with the found center of gravity is shown on fig. 8b. In fig. 8c, the estimated contour around the tumor (white line) is presented. For comparison, the true contour of the modeled object is presented by the black line. On fig. 10, the errors of the modeled contour are presented. It can be seen that there are errors greater than 2.5 [mm]. On fig. 9, the histogram of the intensities of the image is presented and the determined threshold is marked on the x-axes with the symbol 'x'.

The results for the denoised image are presented on figures fig. 11a, fig. 11b and fig. 11c correspondingly. The automatically determined seed point (fig. 11b) is used for the tracking algorithm for tumor segmentation. It can be seen that the errors are decreased to the level under 1.5 [mm].

Two real images are processed by the proposed algorithm. The results obtained are presented on fig. 14 and fig. 15.

On fig. 14, a real ultrasound image of a heart is shown. The region of interest (ROI) is selected by using MATLAB Graphical User Interface (GUI). For this region, an auxiliary binary image is obtained and the computed center of gravity for the pixels of the region is marked on fig. 14 with 'o'. The received contour is drawn with white line.

On fig. 15, a real ultrasound (US) image of a breast cyst [14] and the obtained results, achieved by analogical operations, are shown.

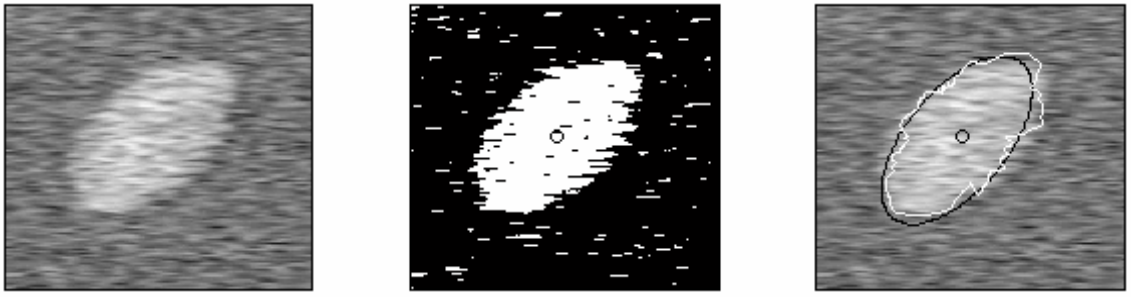

a) Image with lesion area b) Auxiliary binary image c) Contour around lesion area

Fig. 2 Results for image with lesion – ellipse

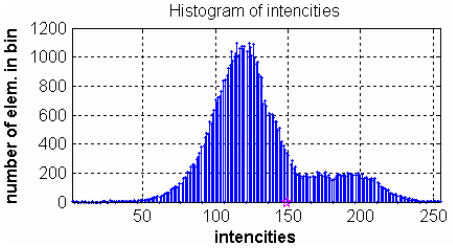

Fig.3 Histogram of image with ellipse

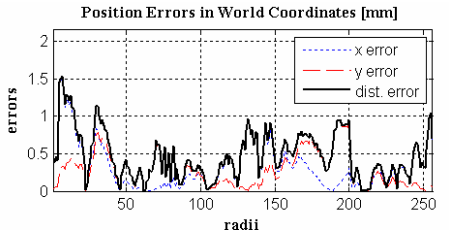

Fig.4. Contour position errors

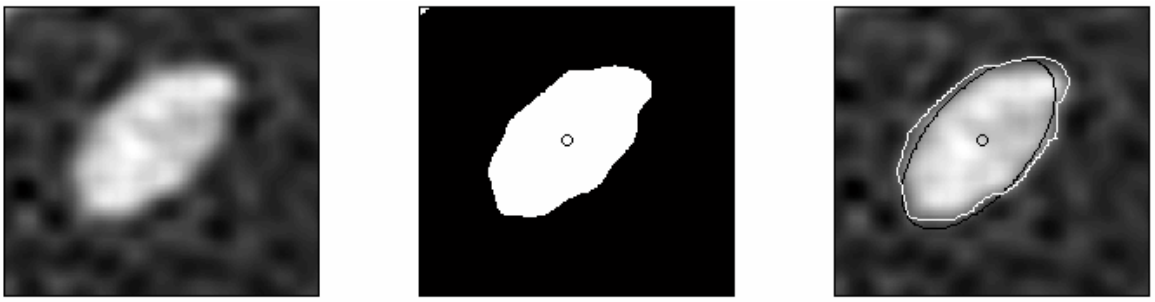

a) Image with lesion area b) Auxiliary binary image c) Contour around lesion area

Fig.5 Results for denoised image with lesion – ellipse

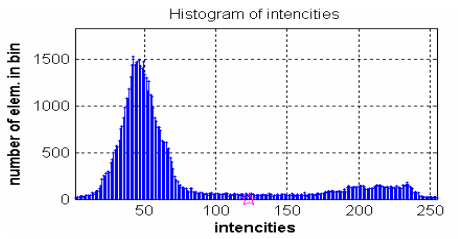

Fig.6 Histogram of denoised image (ellipse)

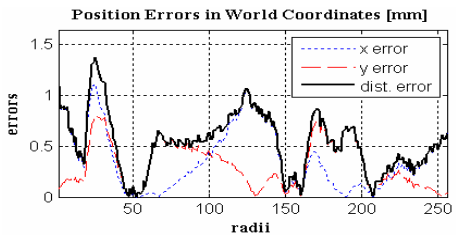

Fig.7. Contour position errors of ellipse

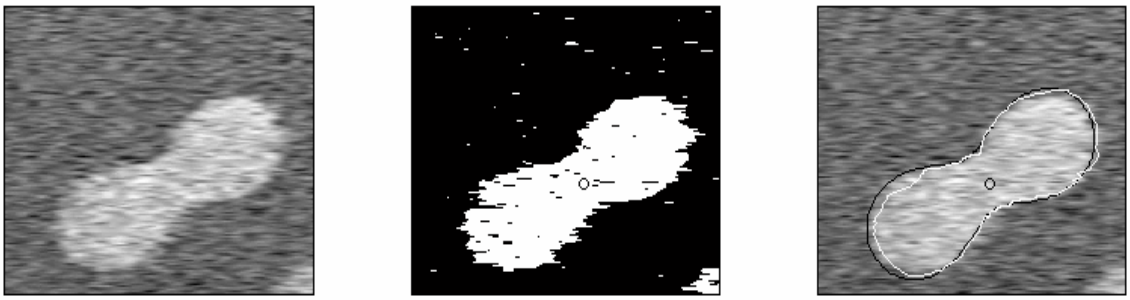

a) Image with lesion area b) Auxiliary binary image c) Contour around lesion area

Fig.8 Results for image with lesion - oval Cassini

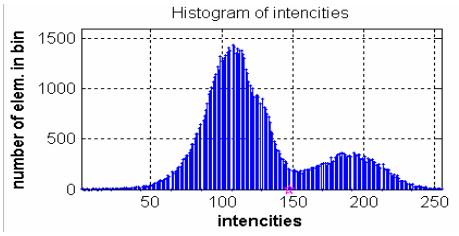

Fig.9 Histogram of image (oval Cassini)

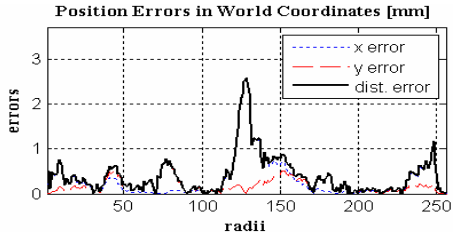

Fig.10. Contour position errors

a) Image with lesion area b) Auxiliary binary image c) Contour around lesion area

Fig.11. Results for denoised image with lesion - oval Cassini

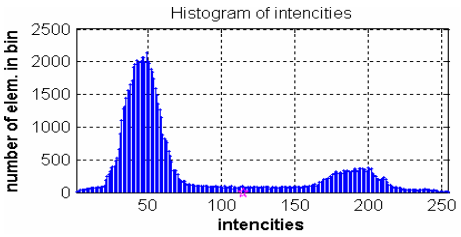

Fig.12 Histogram of denoised image (oval Cassini)

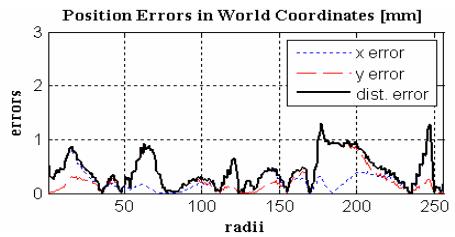

Fig.13. Contour position errors of denoised image (oval Cassini)

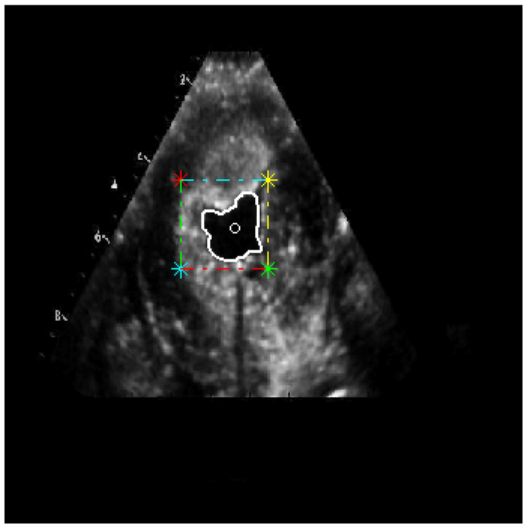

Fig.14 Real image of a heart with specified ROI

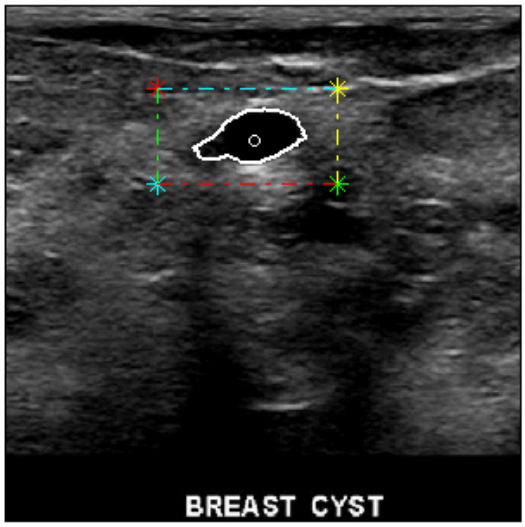

Fig.15 Real image of a breast cyst with specified ROI

5 Conclusion

A new method for automated selection of the internal seed point for convex object segmentation in ultrasound images is proposed. The method uses an auxiliary binary image produced by thresholding of the original image. The assumptions are that the objects have convex form and that the image contains two main classes of intensities: one - for the object and the other - for the background. The threshold is determined by using the Otsu algorithm for threshold determination. The center of gravity of the pixels of the object class is calculated and used as an internal seed point. The method is illustrated by simulating ultrasound images with known true contours of the objects. The estimated contour errors are shown to be mainly less than 1 [mm]. Two real medical images are also processed by the proposed algorithm and the corresponding results are shown.

Acknowledgement: This work is partially supported by the Bulgarian Foundation for Scientific Investigations: MI-1506/05 and VU-MI-204/06.

References:

[1] Abolmaesumi, P., Sirouspour, M.R.: *An Interacting Multiple Model Probabilistic Data Association Filter for Cavity Boundary Extraction from Ultrasound Images*, IEEE trans. on Medical Imaging, vol.23, No 6, June (2004) 772-784

[2] Angelova D., Mihaylova L., *Contour Extraction from Ultrasound Images Viewed As a Tracking Problem*, 12th International Conference on Information Fusion, Seattle, WA, USA, July 6-9, 2009, pp. 284-291 , 978-0-9824438-0-4 ©2009 ISIF.

[3] Bar-Shalom Y., Li X.R., Kirubarajan T. (2001). *Estimation with Applications to Tracking and Navigation: Theory, Algorithms and Software*. Wiley, New York.

[4] Jensen J.A.: Field: *A Program for Simulating Ultrasound Systems*, Paper presented at the 10th Nordic-Baltic Conference on Biomedical Imaging Published in Medical & Biological Engineering &

Computing, pp. 351-353, Vol. 34, Supplement 1, Part 1, 1996.
http://server.oersted.dtu.dk/personal/jaj/field/

[5] Jensen J. A. and N. B. Svendsen: *Calculation of pressure fields from arbitrarily shaped, apodized, and excited ultrasound transducer*s, IEEE Trans. Ultrason., Ferroelec., Freq. Contr., 39, pp. 262-267, 1992. (visited 19.05.2008)

[6] Konstantinova P., D. Adam, D. Angelova and V. Behar, *Contour Determination in Ultrasound Medical Images Using Interacting Multiple Mode Probabilistic Data Association Filter*, Springer-Verlag,2007, LNCS 4310, pp.628-636.

[7] Nacereddine N., L. Hamami, M. Tridi, and N. Oucief, Non-Parametric Histogram-Based *Thresholding Methods for Weld Defect Detection in Radiography*, World Academy of Science, Engineering and Technology ,9, 2005, pp. 213-217.

[8] Nikolov M., P. Konstantinova and V. Behar, *An Improvement of a Probabilistic Based Image Segmentation Algorithm for Ultrasound Medical Images*, International Conference, Automatics and Informatics, 3-6 Oct. 2007, Sofia, Bulgaria VII-9 to VII-12

[9] Noble J. A., Boukerroui D., "*Ultrasound Image Segmentation: A Survey*", IEEE Trans. Medical Imaging,Vol. 25, No. 8, pp. 987–1010, 2006.

[10] Konstantinova P., Nikolov M., Behar V., "*Ultrasound Image Enhancement via Wavelet Thresholding*", International Conference "Automatics and Informatics'08" , Sofia, October 1-4 2008, pp. IV-5 до IV-8, ISSN 1313-1850

[11] Kingsbury N. G., "*A dual-tree complex wavelet transform with improved orthogonality and symmetry properties*", Proceedings of the IEEE Int. Conf. on Image Proc. (ICIP), 2000, http://taco.poly.edu/WaveletSoftware (visited 19.11.2008)

[12] Kirubarajan T., Bar-Shalom Y., (2004). *Probabilistic Data Association Techniques for Target Tracking in Clutter*, Proc. of the IEEE, vol.92, No 3, march, pp. 536-557.

[13] Selesnick I., R. Baraniuk, and N. Kingsbury, *The Dual-Tree Complex Wavelet Transform*, IEEE Signal Processing Magazine, Nov. 2005, pp.123-151.

[14] http://smiswi.sasktelwebhosting.com/ultrasound.htm#BreUS#BreUS (US breast image) (visited 18.08.09)

VERA BEHAR
Institute for Parallel Processing (IPP) - Bulgarian Academy of Sciences (BAS), Department of Mathematical Methods for Sensor Information Processing.
Address: Institute for Parallel Processing, BAS, "Acad. G. Bonchev", Str., bl.25-A, 1113 Sofia, BULGARIA.
E-mail: behar@bas.bg

PAVLINA KONSTANTINOVA
Institute for Parallel Processing (IPP) - Bulgarian Academy of Sciences (BAS), Department of Mathematical Methods for Sensor Information Processing.
Address: Institute for Parallel Processing, BAS, "Acad. G. Bonchev", Str., bl.25-A, 1113 Sofia, BULGARIA.
E-mail: pavlina@bas.bg

MILEN NIKOLOV
Institute for Parallel Processing (IPP) - Bulgarian Academy of Sciences (BAS), Department of Mathematical Methods for Sensor Information Processing.
Address: Institute for Parallel Processing, BAS, "Acad. G. Bonchev", Str., bl.25-A, 1113 Sofia, BULGARIA.
E-mail: milenik@bas.bg